Dodecyl amine adsorption at different interfaces during bubble attachment/detachment at a silica surface

Xuming Wang, Jan D. Miller

University of Utah, College of Mines and Earth Sciences, Department of Metallurgical Engineering, 135 South 1460 East, Rm 412, Salt Lake City, UT 84112

Corresponding author: jan.miller@utah.edu (Jan D. Miller)

Abstract: The reverse flotation of quartz and other gangue silicate minerals with alkyl amines is an important and well known strategy for the processing of iron ore, low grade bauxite ore, and phosphate rock. Some details of amine adsorption by quartz have been described in the literature, but little is known about the disposition of amine during bubble attachment. Now, a new experimental procedure involving vibrational sum frequency spectroscopy (VSFS) has been developed to provide, for the first time, a more detailed analysis of the state of dodecyl amine (DDA) adsorption at different interfaces during bubble attachment/detachment at a silica surface. The results show that the hydrophobic surface state at the silica surface is created by the transfer of a well-organized monolayer of DDA from the bubble surface to the silica surface during bubble contact and attachment.

1. Introduction

Adsorption of amines at different mineral surfaces has been studied extensively (Chernyshova et al., 2001; Koua et al., 2010). The interaction of bubbles with solid surfaces is an important phenomenon in many areas of technology, particularly in flotation technology (Nguyen et al., 1997; Krasowska and Malysa, 2007; Parkinson and Ralston, 2011). Such understanding regarding bubble attachment/detachment is crucial for the development and/or optimization of new flotation technology including the influence of adsorbed surfactants (Nguyen and Stechemesser, 2004; Albijanic et al., 2012).

Previous research on dodecyl amine adsorption at a silica surface using vibrational sum frequency spectroscopy (VSFS) revealed the nature of the adsorbed amine as a function of pH (Wang et al., 2010). Transport and adsorption of collectors to create a hydrophobic surface state have always been of interest to flotation chemists. For soluble collectors the transport and adsorption of the collector are generally thought to occur by diffusion and surface reaction, creating a hydrophobic state at the mineral surface. In some cases the adsorption of collector at the mineral surface may be facilitated by air bubbles. Specifically, in the case of amine flotation of quartz, it has been reported that adsorption of amine increases significantly in the presence of air bubbles. Digre and Sandvik in their experiments with hydrochlorides of C12, C14, and C16 primary amines demonstrated that adsorption at the quartz surface more than doubled when the conditioning of the quartz suspensions was carried out in the presence of gas bubbles (Digre and Sandvik, 1968). Vibrational sum frequency spectroscopy (VSFS) results reported herein confirm this phenomenon and provide further insights regarding amine transport and distribution during air bubble attachment/detachment.

VSFS is a technique for the investigation of surfaces and interfaces (Shen, 1984). As a second order nonlinear optical process VSFS exploits the symmetry breaking at the interface between two isotropic media, which gives rise to a nonlinear susceptibility $\chi^{(2)}$. For the VSFS experiment, the spatial and temporal combination of photons from a tunable IR (ω_{IR}) radiation and photons from a fixed

frequency visible (ω_{Vis}) radiation interact at the surface. As a result, a third photon is produced having a frequency which is the sum of the two incident frequencies ($\omega_{SF} = \omega_{IR} + \omega_{Vis}$). The effective nonlinear polarization has the form (Guyot-Sionnest et al., 1987):

$$P(\omega_{SF}) = \chi^{(2)}E(\omega_{IR})E(\omega_{Vis}), \tag{1}$$

where $E(\omega_{IR})$ and $E(\omega_{Vis})$ are the incident light fields. Generally, the visible frequency is chosen to be off resonance, thus the $\chi^{(2)}$ only depends on the IR frequency.

The obtained VSFS spectra are of the form:

$$I_{SF} \propto |P_{SF}|^2 \propto \left|\chi^{(2)}\right|^2 I_{Vis}I_{IR}f_{Vis}^2 f_{IR}^2 f_{SF}^2, \tag{2}$$

where I_{Vis} and I_{IR} are the intensities of the incident beams, the *f* terms are the Fresnel factors that can be considered constants for a small frequency band (Schroedle et al., 2007). The $\chi^{(2)}$ can be treated as a nonresonant part $\chi_{NR}^{(2)}$ and a resonant component of the susceptibility $\chi_R^{(2)}$:

$$\chi^2 = \chi_R^{(2)} + \chi_{NR}^{(2)}. \tag{3}$$

We can consider an adsorbed monolayer on a dielectric substance, such as silica. In this instance, $\chi_{NR}^{(2)} = 0$, and consequently, the spectrum obtained is purely that of the resonant susceptibility. The resonant component is given by:

$$\chi_R^{(2)} = N\left(\sum_{x=1}^{m} \frac{\langle A_k M_{ij}\rangle_x}{\omega_{v_x} - \omega_{IR} - i\Gamma}\right) \tag{4}$$

where *m* is the number of vibrational transitions, A_k and M_{ij} are the IR and Raman transition probabilities, respectively, ω_{v_x} is the normal mode vibrational frequency of the transition being probed, and Γ is the line width of the transition. The average orientation of interfacial molecules can be obtained from $\chi^{(2)}$ by appropriate choice of input and output polarizations, namely: *ssp* (*s*-polarized sum-frequency, *s*-polarized visible and *p*-polarized IR) and *sps* (*s*-polarized sum-frequency, *p*-polarized visible and *s*-polarized IR), where the letter *s* represents light polarized perpendicular to the plane of incidence and the *p* parallel to the plane of incidence. The spectrum analysis can be made by using amplitudes determined from the fits of the VSFS spectra in Eq. (4).

2. Materials and methods

2.1 Materials

All solutions were prepared using > 18.2 MΩ·cm water from a Millipore water purification system. Dodecyl amine hydrochloride (99%, Acros), and NaOH (98%, Mallinckrodt) were used as received for pH adjustment. An IR/UV grade fused silica hemicylindrical prism (Almaz Optics, Marlton, NJ) was used as the substrate for all VSFS experiments.

2.2 VSFS experiments

An EKSPLA, Ltd. sum-frequency vibrational spectrometer was used for the silica/amine solution experiments. The laser system has been described in a previous publication (Wang et al., 2010), so a description is not provided here. The incident angles of the visible and IR beams at the silica/solution interface were set at 60° and 66°, respectively, and the SF signal was collected in reflection at an angle of 65°. The pulse energies of the visible and the IR beams were 500 and 160 μJ, respectively, for 3200 cm^{-1} at the sample interface.
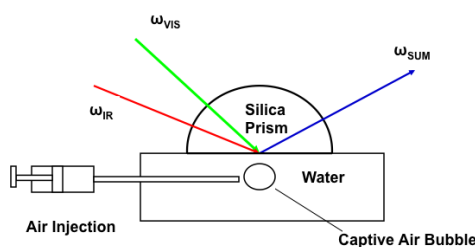

Fig. 1. Experimental set-up to measure VSFS spectra of water films created with a captive bubble at hydrophilic and hydrophobic silica surfaces

A water sample cell (Fig. 1) with an air bubble screw holder was used to conduct the VSFS experiments with the EKSPLA, Ltd. sum-frequency vibrational spectrometer. The spectra presented were taken under *ssp* polarization conditions for the three beams (*s*-polarized sum-frequency, *s*-polarized visible and *p*-polarized IR). Data were collected at 4 cm^{-1} increments, and each point is the average of 30 laser shots. All spectra were recorded at a constant temperature of 23 °C.

3. Results

3.1 Before bubble attachment

It is well known that excellent quartz flotation is achieved from pH 9-10 with dodecyl amine (DDA) at a concentration of 4×10^{-5} M (Fuerstenau, 1957). At lower DDA concentrations flotation recovery of quartz is reduced and the contact angle decreases from ~80° at 4×10^{-5} M to ~35° at 1×10^{-5} M (Fuerstenau, 1957; Smith, 1962). The corresponding DDA adsorption density at 1×10^{-5} M has been reported to be quite low, about 4×10^{-12} moles/cm^2 (Li, 1958). This low adsorption density is confirmed from VSFS experiments together with the surface state of adsorbed DDA. For example, the VSFS spectrum shown in Fig. 2 suggests little, if any, DDA adsorption. The CH vibrations (2800-2940 cm^{-1}) are not detected and the silica surface is characterized by the OH vibrations of interfacial water molecules (3200 and 3500 cm^{-1}). The extent of DDA adsorption by silica at pH 9.6 and 1×10^{-5} M DDA is rather small.
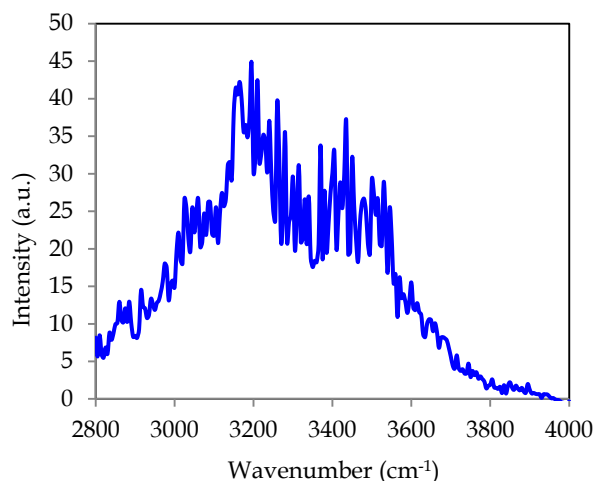

Fig. 2. VSFS spectrum for 1×10^{-5} M DDA solution/silica interface at pH 9.6

Adsorption of DDA at the air/solution interface can be compared to adsorption at the silica surface from surface tension measurements. The results from surface tension measurements are presented in Fig. 3 and the adsorption density is calculated from the Gibbs adsorption equation:

$$\Gamma = -\frac{1}{2.303RT}\left(\frac{\partial \gamma}{\partial \log C}\right), \tag{5}$$

where Γ is the adsorption density, R is the gas constant, T is the temperature, γ is the surface tension, and C is the amine concentration. In this way, the adsorption density at the air/solution interface is found to be quite significant, 5.26×10^{-10} moles/cm^2, corresponding to monolayer coverage of DDA. Thus, adsorption at the air bubble surface is expected to be about 100 times greater than adsorption at the silica surface.

These results for DDA adsorption at the air/solution interface are supported by VSFS analyses which show strong CH$_3$ vibrations (2875 and 2940 cm^{-1}) and the exclusion of interfacial water molecules (Fig. 4a). Further, the order and conformation of the dodecyl chain can be analyzed from the spectrum shown in Fig. 4. If the VSFS spectrum originates from a well-packed monolayer of dodecyl amine with the hydrocarbon chain in the all-trans state only the CH$_3$ symmetric stretching mode (2875 cm^{-1}) and CH$_3$ Fermi stretching mode (2940 cm^{-1}) from the terminating methyl groups will be observed for the *ssp* polarization combination. The VSFS spectrum in Fig. 4a and the surface

tension results presented in Fig. 3 suggest that the DDA molecules are present as a well-ordered monolayer at the air/water interface at a concentration of 4×10^{-5} M. At the DDA concentration of 1×10^{-5} M (Fig. 4b) the VSFS spectra show a CH_2 stretching peak at 2850 cm^{-1} which indicates that the adsorbed DDA monolayer at the air/solution interface at this concentration has some gauche defects.

In summary, under these conditions (pH 9.6, DDA = 1×10^{-5} M) before bubble attachment, DDA is not present in a significant amount at the silica surface, or, if present, adsorbed amine is at a low adsorption density in random organization. In contrast, amine is organized at the air/solution interface (pH 9.6, DDA = 4×10^{-5} M) as a well-ordered monolayer with some gauche defects.
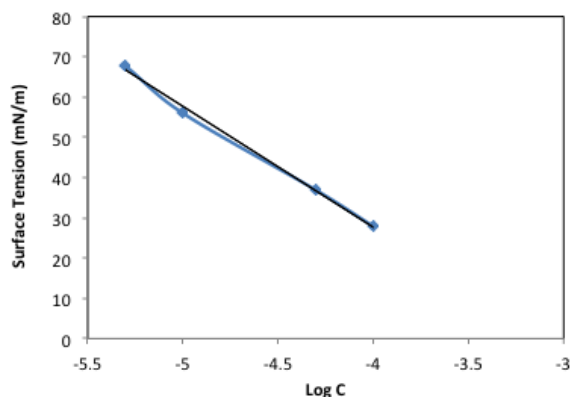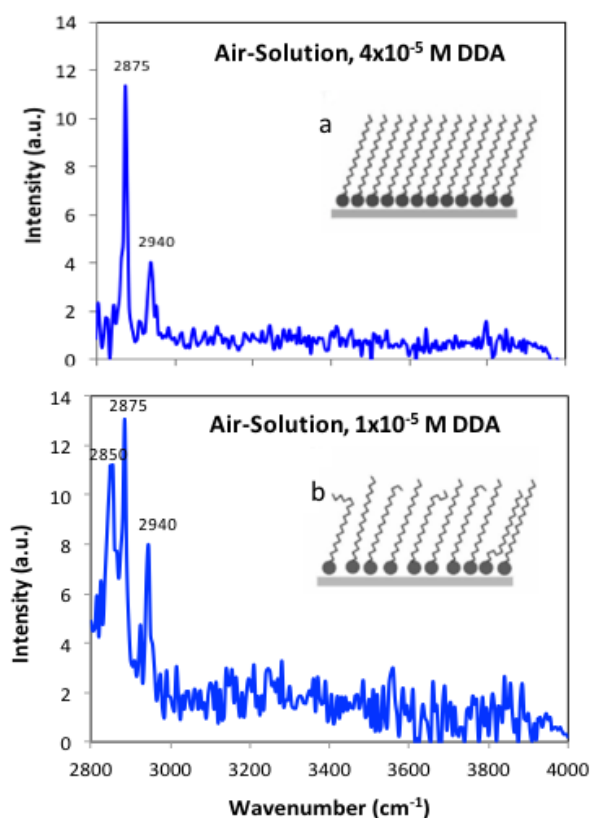

Fig. 3. Surface tension for a DDA solution at pH 9.6

Fig. 4. VSFS spectra of the air/DDA solution for 4×10^{-5} and 1×10^{-5} M DDA concentration at pH 9.6

3.2 During bubble attachment

The most interesting result is that the VSFS spectrum of the quartz surface at pH 9.6 and DDA concentration of 1×10^{-5} M, is transformed during bubble attachment so that, instead of the spectrum

shown in Fig. 2, transfer of DDA occurs and the spectrum of the quartz surface now shows strong ordered adsorption of DDA similar to that structure which was observed at the air/solution interface. So, even though little DDA is adsorbed at the silica surface, bubble attachment occurs in captive bubble experiments and a contact angle of 64° is observed at pH 9.6 and a DDA concentration of 1×10^{-5} M. After film rupture and stabilization of an equilibrium contact angle, the VSFS results for the silica surface with an attached air bubble are presented in Fig. 5. Notice the shape of the spectrum is quite different from the spectrum for the air/solution interface shown in Fig. 4-a, but is similar to that shown in Fig. 4-b. In addition to the CH_3 stretching peaks at 2875 and 2940 cm^{-1} there are two peaks near 2850 and 2920 cm^{-1}. The OH stretching modes are also found in the spectrum near 3200 and 3500 cm^{-1}. Some residual water was observed at the surface after film rupture as shown by a photograph taken through the silica substrate after bubble attachment (see Fig. 6). Therefore, even though the spectrum clearly shows that DDA has been stabilized as an ordered monolayer at the air bubble/silica surface and that the peaks associated with the CH vibrations of adsorbed DDA are of significantly greater intensity, the adsorbed layer has a different structure than that observed for the well-ordered monolayer at the air/DDA solution interface (4×10^{-5}M). In order to further analyze the conformation of the adsorbed DDA layer at the quartz surface during bubble attachment (Eq. 2) was used to fit the spectrum in Fig. 5 for the CH stretching range.
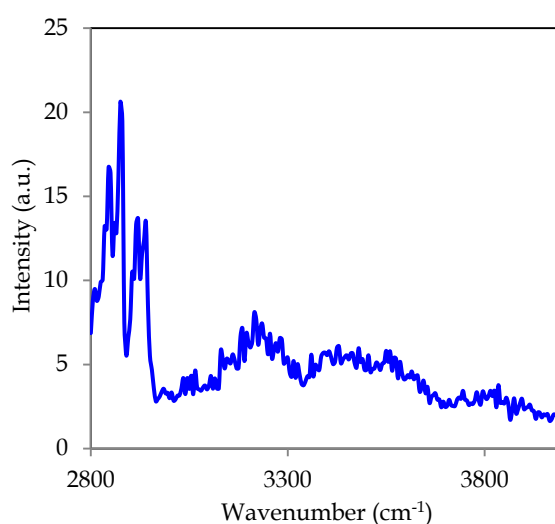

Fig. 5. VSFS spectrum after air bubble attachment for a 1×10^{-5} M DDA solution at pH 9.6
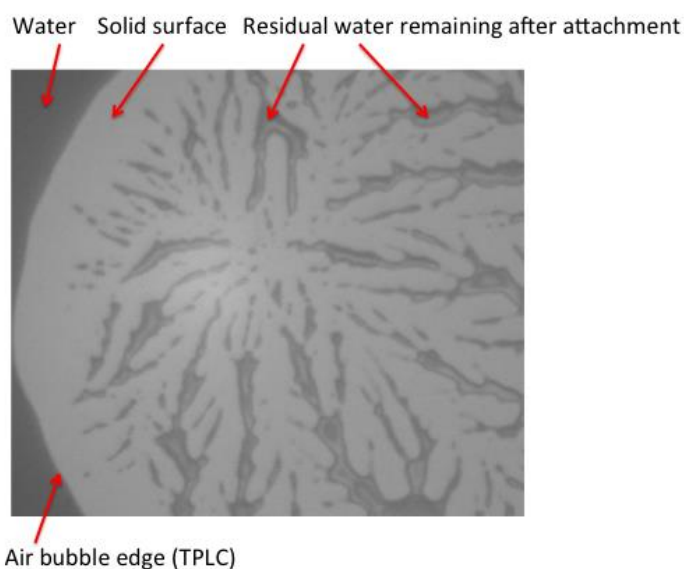

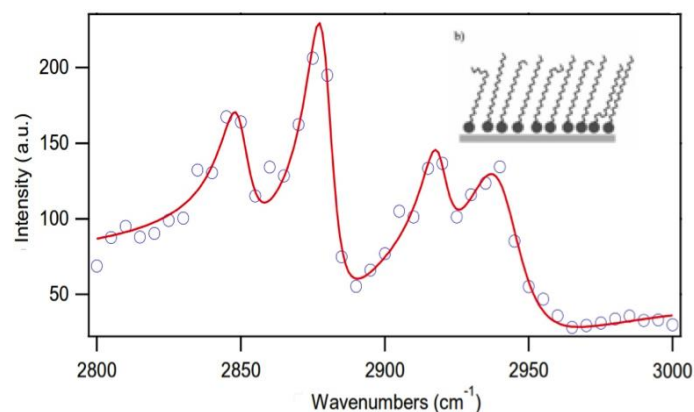Fig. 6. Photograph of residual water at the surface after film rupture

Fig. 7. Fitted VSFS spectrum in the CH stretching range using Eq. (2)

The fitted spectrum in the CH stretching range can be seen from Fig. 7. The two CH_2 stretching modes are clearly revealed at 2848 cm^{-1} for the CH_2 symmetric stretching mode and at 2920 cm^{-1} for the CH_2 asymmetric stretching mode. It is evident that the DDA has been transferred to the silica surface during film rupture and bubble attachment. The CH_2 mode indicates an adsorbed DDA layer containing some isolated gauche defects. VSFS of the silica surface with an attached bubble reveals that more ordered DDA molecules are present at the silica surface as evidenced by significant CH stretching peaks in Fig. 5 after bubble attachment compared to before bubble attachment (no significant CH stretching peaks appear in Fig. 2). A less ordered monolayer due to increased gauche defects (compared to that at the air/water interface in Fig. 4) may be formed at the bubble/silica interface.

3.3 After bubble detachment

Finally, as shown in Fig. 8, after bubble removal, the silica surface is stripped of most of the DDA and water is dominant again at the silica surface. Notice that there is some residual DDA as evidenced by the peaks for CH vibrations at 2865 and 2930 cm^{-1}. However, most of the surface is occupied by water molecules as revealed by the OH peaks at 3215 and 3455 cm^{-1}.
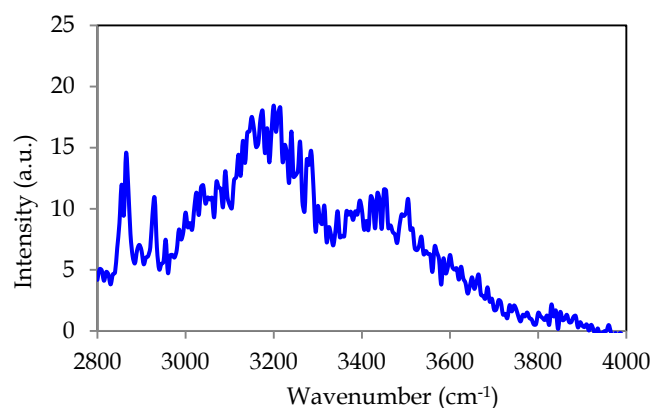

Fig. 8. VSFS spectrum for 1×10^{-5} M DDA solution/silica interface at pH 9.6 after bubble detachment

4. Discussion

As mentioned previously, for soluble collectors the transport and adsorption of collector is generally thought to occur by diffusion and surface reaction, creating a hydrophobic state at the mineral surface. In some cases, adsorption of collector at the mineral surface may be facilitated by air bubbles. Specifically, in the case of amine flotation of quartz it has been reported that adsorption of amine increases significantly in the presence of air bubbles. Digre and Sandvik (1968) in their experiments with hydrochlorides of C12, C14, and C16 primary amines demonstrated that adsorption at the quartz

surface was more than doubled when the conditioning of the quartz suspensions was carried out in the presence of gas bubbles. In a recent paper Laskowski (2013) proposed that when amine collector is added to the saturated brine during soluble salt flotation, amine precipitates are formed and coat the bubble (air/water) interface forming a molecular film. The paper concluded that the amine coated bubble starts spreading into a molecular film that activates the bubbles with regard to their ability to attach to the surface of the KCl particles. Although the paper indicated that the presence of a stable air bubble increases the proportion of the amine which acts as an active component in the potash ore flotation, the study did not explain how the activated bubbles attach to the KCl particles. The results from our study may help answer this question.

At pH 9.6 the silica surface is negatively charged and at low dodecyl amine concentrations the dodecyl ammonium ions are adsorbed as individual ions at the low adsorption density. The system is characterized by its hydrophilic state as revealed from the literature (Li, 1958) and by results from VSFS spectroscopy in Fig. 2.

Under these conditions, the limited adsorption at the amine solution/silica interface is accompanied by good DDA adsorption at the air bubble/amine solution. During bubble attachment, DDA is transferred to the quartz surface and the adsorption density increases significantly with the formation of an ordered monolayer at the air bubble/silica interface as established from VSFS analysis in Fig. 5, and as shown by the illustrations presented in Fig. 9.

Fig. 9. Illustration of DDA molecules transferred to the quartz surface during bubble attachment

Thermodynamic analysis (de Bruyn and Aga, 1962) of bubble attachment shows that if a solid were to become floatable, the adsorption density of the collector at the solid-gas interface must exceed its adsorption density at the solid-liquid interface.

According to the Gibbs equation, for the solid-liquid interface:

$$d\gamma_{SL} = -\Gamma_R^{SL} d\mu_R \tag{6}$$

for the solid-gas interface:

$$d\gamma_{SG} = -\left(\Gamma_R^{SG} - \alpha\Gamma_{H_2O}^{SG}\right) d\mu_R \tag{7}$$

and

$$d(\gamma_{SG} - \gamma_{SL}) = -\left[\Gamma_R^{SG} - \alpha\Gamma_{H_2O}^{SG} - \Gamma_R^{SL}\right] d\mu_R \tag{8}$$

for an increase in the contact angle:

$$\Gamma_R^{SG} > \Gamma_R^{SL} + \alpha\Gamma_{H_2O}^{SG} \tag{9}$$

where γ_{SL} is the interfacial tension for the solid/liquid interface, γ_{SG} is the interfacial tension for the solid/gas interface, Γ_R^{SG} is the collector R adsorption density at the solid/gas interface, Γ_R^{SL} is the collector R adsorption at the solid/liquid interface, $\Gamma_{H_2O}^{SG}$ is the water adsorption density at the solid/gas interface, and μ_R is the chemical potential for collector R. Thus, the adsorption density of the DDA must be greater at the air/quartz interface than at the DDA solution/quartz interface for the contact angle to increase as has been demonstrated qualitatively from VSFS.

Prior to bubble contact at the silica surface, little DDA adsorption occurs at the silica surface for 1×10^{-5} M DDA, whereas DDA monolayer adsorption occurs at the air bubble surface. When the air bubble contacts the silica surface, bubble film rupture and attachment occur. The DDA molecules are transferred to the silica surface as shown in Fig. 9. The DDA adsorption density at the air/silica interface is greater than at the solution/silica interface which agrees with the thermodynamic analysis for successful attachment.

5. Conclusions

VSFS evidence has been presented which shows that bubble attachment at a quartz surface from a 1×10^{-5} M DDA solution at pH 9.6 is accomplished by the transfer of a well ordered DDA monolayer from the air/solution interface to the air/quartz interface during film rupture and bubble attachment. These results are consistent with the thermodynamic analysis that bubble attachment and formation of a stable contact angle occurs when the DDA adsorption density at the air/quartz interface exceeds the DDA adsorption density at solution/quartz interface.

Acknowledgements

References

ALBIJANIC, B., BRADSHAW, D. J., NGUYEN, A. V., 2012. *The relationships between the bubble-particle attachment time, collector dosage and the mineralogy of a copper sulfide ore*. Minerals Engineering, 36–38, 309–313.

CHERNYSHOVA, I. V., HANUMANTHA Rao, K., VIDYADHAR, A., 2001. *Mechanism of adsorption of long-chain alkylamines on silicates: A spectroscopic study. 2. Albite*. Langmuir, 17, 775-785.

DIGRE, M., SANDVIK, K.L., 1968. *Adsorption of amine on quartz through bubble interaction*. IMM Transactions, Section C, 77, C61-64.

DE BRUYN, P.L., AGA, G.E., 1962. Surface chemistry of flotation. In: *Froth flotation-50th anniversary*. Fuerstenau, D.W. (ed.), American Institute of Mining, Metallurgical, and Petroleum Engineers, New York, NY, USA, 91-138.

FUERSTENAU, D.W., 1957. *Correlation of contact angle, adsorption density, zeta potentials and flotation rate*. AIME Transactions, 208, 1365-1367.

GUYOT-SIONNEST, P., HUNT, J.H., SHEN, Y.R., 1987. *Sum-frequency vibrational spectroscop of a Langmuir film: Study of molecular orientation of a two-dimensional system*. Physical Review Letters, 59(14), 1597-1600.

KRASOWSKA, M., MALYSA, K., 2007. *Wetting films in attachment of the colliding bubble*. Advances in Colloid and Interface Science, 134–135, 138–150.

KOUA, J. Ko, TAO, D., XUA, G., 2010. *A study of adsorption of dodecylamine on quartz surface using quartz crystal microbalance with dissipation*. Colloids and Surfaces A: Physicochemical and Engineering Aspects, 368, 75–83.

LASKOWSKI, J. S., 2013. *From amine molecules adsorption to amine precipitate transport by bubbles: A potash ore flotation mechanism*. Minerals Engineering, 45, 170–179.

LI, H., 1958. *Adsorption of organic and inorganic ions on quartz*. Doctoral Thesis, Massachusetts Institute of Technology, Cambridge, MA, USA.

NGUYEN, A. V., SCHULZE, H. J., RALSTON, J., 1997. *Elementary steps in particle-bubble attachment*. International Journal of Mineral Processing, 51, 183–195.

NGUYEN, A. V., STECHEMESSER, H., 2004. *Influence of dewetting kinetics on bubble-particle interaction*. Physical Chemistry Chemical Physics, 6, 429–433.

PARKINSON, L., and RALSTON, J., 2011. *Dynamic aspects of small bubble and hydrophilic solid encounters*. Advances in Colloid and Interface Science, 168, 198–209.

SCHROEDLE, S., MOORE, F.G., RICHMOND, G.L., 2007. *Surface speciation at solid/liquid interfaces: A vibrational sum-frequency study of acetate at the fluorite/water interface*. Journal of Physical Chemistry C, 111, 10088-10094.

SHEN, Y.R., 1984. *The principles of nonlinear optics*. Wiley, New York, NY, USA.

SMITH, R.W., 1962. *Contact angles in a quartz dodecylammonium acetate solution-nitrogen system*. Proceedings South Dakota Academy of Science, XLI, 150.

WANG, X., LIU, J., DU, H., and MILLER, J.D., 2010. *States of adsorbed dodecyl amine and water at a silica surface as revealed by vibrational spectroscopy*. Langmuir, 26(5), 3407–3414.